# EMITTANCE OF A LOW-POWER RF ION SOURCE WITH A MICROMETER-SCALE EXTRACTION APERTURE

Vitalii I. Voznyi*, Aleksandr G. Ponomarev, Dmytro V. Mahilin, Dmytro P. Shulha, Volodymyr A. Rebrov

*Institute of Applied Physics NAS of Ukraine, 58, Petropavlivska Str., 40000 Sumy, Ukraine*
*Corresponding Author: vozny56@gmail.com*

The concept of a compact nuclear microprobe is based on specialized ion sources with beam currents not exceeding a few nanoamperes and a small energy spread. At the Institute of Applied Physics, NAS of Ukraine, a low-power RF ion source has been developed for application in a compact nuclear microprobe. The source operates at low RF power (< 10 W) and is designed to generate a $^1H^+$ ion beam required for standard techniques such as PIXE, RBS, and proton beam writing. To reduce the beam emittance and improve the spatial resolution of the microprobe, the source extraction aperture diameter was reduced to 50 μm. This paper reports measurements of the total beam current and emittance extracted from the low-power RF ion source with a micrometer-scale extraction aperture. Data on the beam profile, its diameter, and divergence angle are also presented. The main parameters of the RF source are as follows: quartz chamber diameter – 34 mm, length – 70 mm, working gas – hydrogen, extraction aperture diameter – 50 μm, RF power ≤ 10 W, frequency – 45 MHz, ion current up to 100 nA. The extraction voltage varies from 10 to 300 V, while the beam energy ranges from 1 to 6.5 keV. Beam emittance was measured using an electrostatic Allison-type scanner. The minimum emittance containing 90% of the total beam current was found to be $\varepsilon_{90}$ = 1.36 π·mm·mrad, while the rms-emittance is $\varepsilon_{rms}$ = 0.32 mm·mrad. The normalized emittance is $\varepsilon_N$ = 0.003 π·mm·mrad, and the energy-normalized emittance equals 0.1 π·mm·mrad·$(MeV)^{1/2}$. It is shown that reducing the diameter of the extraction aperture of the ion source to 50 μm results in a significant improvement in the ion-optical characteristics of the extracted beam.

**Keywords**: *Ion beam; Radiofrequency Ion source; Beam current density; Extractor; Emittance*
**PACS**: 29.25.Ni; 41.75.Ak; 41.85.Qg; 41.85.Ne

Nuclear microprobe facilities are intended for local, non-destructive microanalysis of materials of diverse origin as well as for the fabrication of high-quality micro- and nanostructures. Modern microprobe systems represent one of the analytical channels within multi-purpose complexes based on electrostatic accelerators. These accelerators typically deliver ion beam energies of several MeV and currents up to 100 μA [1–3]. To achieve significant demagnification factors in the ion-optical system, the overall length of the microprobe beamline may extend to about 10 m.

At the Institute of Applied Physics, NAS of Ukraine, a concept for a compact nuclear microprobe has been proposed [4], based on ion sources with beam currents up to 10 nA and an energy spread of about 10 eV.

To achieve high spatial resolution in low-energy (~30 keV) microprobe systems, liquid-metal ion sources, field ion sources [5], or electron-impact ion sources with emission aperture sizes of 0.1–1 μm [6, 7] are commonly employed. However, due to their technical limitations, such sources are not suitable in compact microprobe designs.

In view of this, an inductive RF ion source has been developed at the IAP NAS of Ukraine for application in the injector of a compact nuclear microprobe [8]. The source operates at low RF power (<10 W) and is intended for generating $^1H^+$ ion beams required for standard techniques such as PIXE, RBS, and proton beam writing.

The source operates with hydrogen as the working gas, at an RF power level below 10 W. It is equipped with a 0.6 mm extraction aperture and delivers beam currents up to 3.5 μA with a proton fraction of about 10%. The relatively low RF power enables a reduction of the ion energy spread to 7.5–9 eV. The geometric emittance containing 90% of the total beam current was measured to be $\varepsilon_{90}$ = 9.8 π·mm·mrad, while the energy-normalized emittance of the source equals 0.8 π·mm·mrad·$(MeV)^{1/2}$.

To further enhance the spatial resolution and overall performance of the microprobe, it is essential to extract an ion beam with the lowest possible emittance from the ion source. For this purpose, measurements of the emittance of the ion beam extracted from the low-power RF source with an extraction aperture diameter of 50 μm have been carried out.

This paper presents measurements of the total current and emittance of an ion beam extracted from an RF ion source with a micrometer-scale extraction aperture. Data on the beam profile and divergence angle are also reported.

## RF ION SOURCE AND BEAM CURRENT

The schematic of the inductive RF ion source and its operating principle are described in detail in [8]. The source comprises a cylindrical quartz discharge chamber (Ø 34 mm, length 70 mm) surrounded by a six-turn copper coil. An RF voltage of up to 10 W at 45 MHz is applied to the coil. Hydrogen at ~1 Pa is contained within the chamber. The coil's alternating magnetic field induces an azimuthal RF electric field, which is absorbed by electrons in the gas,

leading to excitation and ionization and forming an RF plasma discharge. Positive ions are extracted by an extraction electrode, while an accelerating electrode focuses the resulting ion beam.

The consumed power of the RF generator is approximately 8 W. Considering the generator efficiency, the RF power absorbed by the plasma does not exceed 5 W.

Fig. 1a shows the dimensions of the extractor with a 50 μm aperture. The aperture is fabricated from platinum.
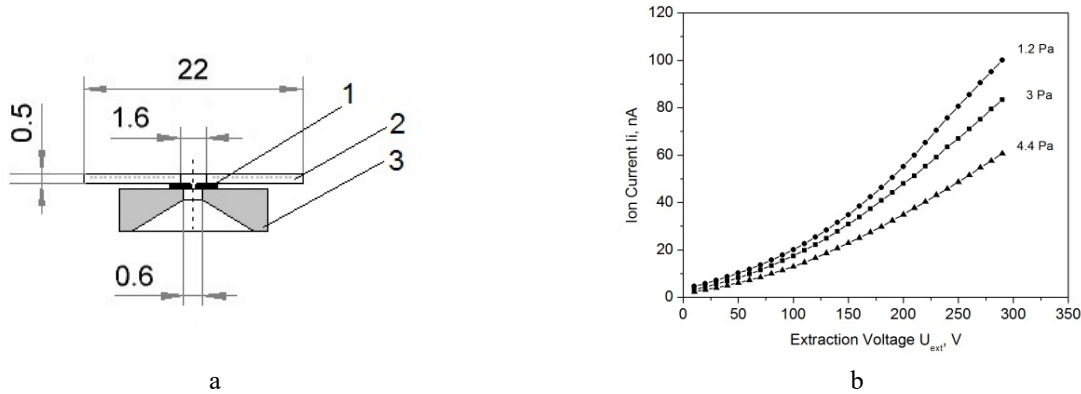


a



b

**Figure 1**. a – extractor with a 50 μm aperture: 1 – aperture, 2 – quartz diaphragm, 3 – extractor. b – ion beam current as a function of extraction voltage for different hydrogen pressures

Measurements of the ion-optical characteristics of the RF source were performed on the experimental setup, the schematic of which is shown in [8]. The ion source was connected to a vacuum chamber with a volume of approximately 6 L, evacuated by a Leybold-360 turbomolecular pump with a pumping speed of 360 L/s. The vacuum chamber was evacuated to a pressure of $1 \times 10^{-4}$ Pa, measured with a VMB-14 magnetic vacuum gauge.

Hydrogen was introduced into the source via a SNA-2 gas supply system. Within the operational range of gas flow, the hydrogen pressure in the source was varied between 0.5 and 5 Pa. Correspondingly, the pressure in the vacuum chamber of the setup ranged from $(3–9) \times 10^{-4}$ Pa.

The current–voltage characteristic of the source, representing the dependence of the ion beam current $I_i$ on the extraction voltage $U_{ext}$, was measured using a Faraday cup located 100 mm from the source. The Faraday cup, with a diameter of 22 mm, was equipped with a suppressor biased at -290 V to eliminate the influence of secondary electrons on the current measurement.

Fig. 1b shows the dependence of the ion beam current $I_i$ on the extraction voltage $U_{ext}$ at different hydrogen pressures in the source chamber in the range of 1.2–4.4 Pa. The extraction voltage $U_{ext}$ was varied from 10 V to 290 V at a constant accelerating voltage of $U_{acc} = 4$ kV.

As seen in Fig. 1b, the ion beam current increases monotonically with extraction voltage and decreases with increasing gas pressure. The maximum current of $I_i$=100 nA is obtained at an extraction voltage of $U_{ext}$=290 V and a low gas pressure of $p$=1.2 Pa.

At a gas pressure of $p$=1.2 Pa, the ion current curve is well approximated by a power-law function $I_i = 5.26 + 4.5 \cdot 10^{-3} \cdot U_{ext}^{1.76}$, where the ion current $I_i$ is expressed in nA and the extraction voltage $U_{ext}$ in Volts. At a pressure of $p$=4.4 Pa, the ion current curve is approximated by the function $I_i = 2.32 + 7.4 \cdot 10^{-3} \cdot U_{ext}^{1.58}$.

This form of the ion current dependence on the extraction voltage is characteristic of plasma ion sources, in which the plasma emission boundary forms a meniscus. The emission boundary changes shape with plasma density $n_e$, electron temperature $T_e$, and extraction voltage $U_{ext}$. The shape of the current–voltage curves is determined by the Child–Langmuir law: $j_i = (4\varepsilon_0/9)\sqrt{2e/m} \cdot (U_{ext}^{3/2}/d^2)$, where $\varepsilon_0$ is the vacuum permittivity, $e$ is the electron charge, $m$ is the electron mass, and $d$ is the distance from the plasma boundary to the extraction electrode.

Since in a plasma source the value of distance $d$ depends on both $n_e$ and $U_{ext}$, the exponent of the power function deviates from the value of 3/2.

The beam current density can be estimated as $j_i = I_i/S_a$, where $S_a$ is the area of the extraction aperture. For $I_i$=100 nA, the current density is $j_i$=5 mA/cm$^2$.

## BEAM EMITTANCE

The RF source's emittance was measured using an electrostatic scanner, whose design and operation are described in detail in [9]. The device is based on the Allison–type scheme [10, 11].

The scanner consists of two parallel deflection plates supplied with a sawtooth voltage, an entrance and exit slit, and a Faraday cup for measuring the ion current transmitted through both slits. The scanner is moved transversely to the beam in the vertical x-direction by a stepper motor. The plates along the beam axis are 120 mm long, with a plate separation of 10 mm. The widths of the entrance and exit slits are 200 μm. The scanner's spatial resolution is 4.8 μm, with a scanning range of 0–20 mm.

The scanner was mounted at a distance approximately 55 mm from the ion source. Scanning along the x-axis was carried out over a range of 0-7 mm with a step size of 93.75 μm. The voltage applied to the deflection plates was varied from -50 V to +50 V in steps of 1 V.

The angular resolution of the scanner depends on the beam energy $E$. For the energy of $E = 6$ keV and a voltage-scanning step of 1 V, the angular resolution is 0.42 mrad.

The determination of the emittance is based on measuring the ion beam intensity distribution $Z(x, x')$ as a function of the coordinate $x$ and angle $x'$. The measured two-dimensional array of ion beam intensity $Z(x, x')$ represents the beam current density distribution in the $x$-$x'$ phase space. The array $Z(x, x')$ enables the determination of key beam parameters: geometric emittance $\varepsilon_{90}$, the rms-emittance $\varepsilon_{rms}$ and the ion beam current profile $Z(x)$.

A cross-section of the distribution $Z(x, x')$ at a given threshold value defines the emittance diagram, the area of which, devided by $\pi$, corresponds to the beam emittance. For a threshold value corresponding to 90% of the total beam current, the resulting emittance diagram represents the contour of the geometric emittance $\varepsilon_{90}$, which encloses 90% of the total beam current.

During beam acceleration, its emittance decreases. The quantity that remains constant under beam acceleration is the normalized emittance, defined as $\varepsilon_N = \varepsilon \cdot \beta \cdot \gamma$, where $\beta$ and $\gamma$ are the relativistic beta and gamma factors. For non-relativistic beams, the expression for the normalized emittance is given by $\varepsilon_N = \varepsilon_{90} \cdot 4,6 \cdot 10^{-5} \sqrt{E/A}$, where $E$ is the beam energy, eV, and $A$ is the ion mass number.

In addition to the geometric interpretation of the emittance as the area of the contour enclosing 90% of all beam particles, there exists a statistical approach in which the beam is considered as a statistical ensemble of points in the two-dimentional phase space $x$-$x'$ [12, 13]. Particles within the space $x$-$x'$ can be treated as a statistical distribution with mean values $\langle x \rangle$ and $\langle x' \rangle$.

In this case, the rms-emittance $\varepsilon_{rms}$ is determined by the standard deviations from these mean values, $\sigma_x$, $\sigma_{x'}$, and $\sigma_{xx'}$, where $\sigma_x^2 = \langle x^2 \rangle$, $\sigma_x^2 = \langle x^2 \rangle$ and $\sigma_{xx'}^2 = \langle xx' \rangle^2$ are the second-order moments of the phase-space distribution function. The expression for calculating the rms-emittance is given by: $\varepsilon_{rms} = \sqrt{\langle x^2 \rangle \langle x'^2 \rangle - \langle xx' \rangle^2} = \sqrt{\sigma_x^2 \sigma_{x'}^2 - \sigma_{xx'}^2}$ .

Emittance measurements of the ion beam were performed for various extraction voltages in the range of $U_{ext}$=150-300 V and acceleration voltages in the range of $U_{acc}$=1.5-6.5 kV. The hydrogen pressure in the source chamber was maintained constant at $p$=1.2 Pa.

Fig. 2a shows the 3D-intensity distribution surface $Z(x, x')$ of the ion beam current, measured at an extraction voltage of $U_{ext}$=280 V and an acceleration voltage of $U_{acc}$=6.0 kV. The corresponding emittance diagram, illustrating the contour of the emittance $\varepsilon_{90}$ enclosing 90% of the total beam current, is shown in Fig. 2b.
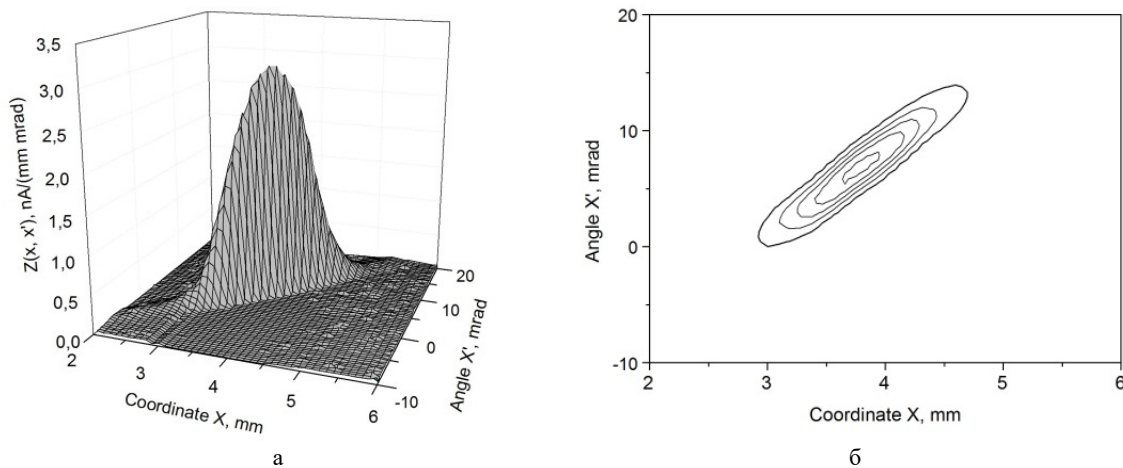


a                                                                       б

**Figure 2.** a – 3D surface of the current intensity distribution $Z(x, x')$, b – contour of $\varepsilon_{90}$ beam emittance

At a beam energy of $E$=6 keV, the geometric emittance was found to be $\varepsilon_{90}$=1.9 $\pi$·mm·mrad. The rms-emittance was $\varepsilon_{rms}$=0.44 mm·mrad. The ratio $\varepsilon_{90}/\varepsilon_{rms}$ is close to the theoretical value of 4.6 for beams with a Gaussian intensity distribution [14, 15]. The normalized emittance was determined to be $\varepsilon_N$=0.0047 $\pi$·mm·mrad for $A$=2.

For comparing the emittances of ion sources with different beam energies, the quantity of the energy-normalized emittance, defined as $\varepsilon \cdot E^{1/2}$, is often used. The energy-normalized emittance of the beam was determined to be 0.15 $\pi$·mm·mrad·(MeV)$^{1/2}$.

The minimum emittance was obtained at an extraction voltage of $U_{ext}$=220 V and an acceleration voltage of $U_{acc}$=5.5 kV. Under these conditions, the geometric emittance was $\varepsilon_{90}$=1,36 $\pi$·mm·mrad, and rms-emittance was $\varepsilon_{rms}$=0.32 mm·mrad, giving ratio $\varepsilon_{90}/\varepsilon_{rms}$=4,2. The normalized emittance was $\varepsilon_N$=0.003 $\pi$·mm·mrad ($A$=2). The energy-normalized emittance was 0.1 $\pi$·mm·mrad·(MeV)$^{1/2}$.
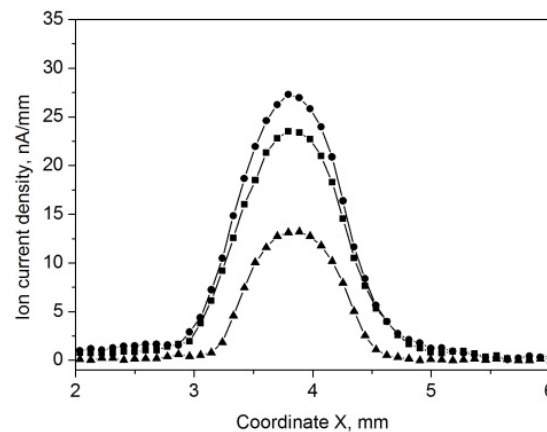
Figure 3 – The current density distribution (beam profile) along the coordinate *x*

The ion beam current profile, or the current density distribution along the coordinate *x*, is obtained by summing the elements of the array $Z(x) = \sum_{x'} Z(x,x')$ over all values of the angle *x´* for each coordinate *x*, resulting in a profile expressed in nA/mm. Figure 3 shows the ion beam profiles measured for three different extraction voltages. The profiles were measured at a distance of approximately 55 mm from the ion source (~120 mm from the extractor).

In the first case, at $U_{ext}$=220 V and $U_{acc}$=5.5 kV, the beam profile is indicated by triangles. The ion beam diameter is $d = 3.2\sigma_x$=1 mm, and the full divergence angle is $\theta = 3.2\sigma_{x'}$=8.3 mrad. The beam emittance is $\varepsilon_{90}$=1.36 π·mm·mrad.

The beam profile, indicated by squares, corresponds to the case, where the extraction voltage is $U_{ext}$=280 V and acceleration voltage is $U_{acc}$=6.0 kV. In this case the beam diameter is $d = 3.2\sigma_x$=1.3 mm, and the divergence angle is $\theta = 3.2\sigma_{x'}$=10.2 mrad. The beam emittance equals $\varepsilon_{90}$=1.9 π·mm·mrad.

In the third case, at $U_{ext}$=300 V and $U_{acc}$=6.5 kV, the beam profile is indicated by dots. The beam diameter is $d = 3.2\sigma_x$=1.4 mm, and the divergence angle is $\theta = 3.2\sigma_{x'}$=11.2 mrad. The beam emittance is $\varepsilon_{90}$=2.0 π·mm·mrad.

## CONCLUSIONS

At the Institute of Applied Physics of NAS of Ukraine, an inductive RF ion source was developed for use in the injector of a compact nuclear microprobe. The source operates at a low RF power of less than 10 W and is designed to generate a $^1H^+$ ion beam required for standard techniques such as PIXE, RBS, and proton-beam writing.

To reduce the ion beam emittance and thereby improve the spatial resolution of the microprobe, the source extraction aperture diameter was reduced from 0.6 mm to 50 μm.

The measurements of the ion-optical beam characteristics showed that:

- the total beam current decreased from 3.5 μA to 100 nA, while the ion current density increased from 1.2 mA/cm² to 5 mA/cm²;
- the geometric emittance was reduced from $\varepsilon_{90}$=9.8 π·mm·mrad to $\varepsilon_{90}$=1.4-2.0 π·mm·mrad;
- the rms-emittance decreased from $\varepsilon_{rms}$=2.2 mm·mrad to $\varepsilon_{rms}$=0.33-0.44 mm·mrad;
- the energy-normalized emittance was 0.1-0.15 π·mm·mrad·(MeV)$^{1/2}$ instead of 0.8 π·mm·mrad·(MeV)$^{1/2}$;
- the ion beam diameter decreased from 3.6 mm to 1-1.4 mm;
- the full beam divergence angle decreased from 30.8 mrad to 8.3-11.2 mrad.

Thus, reducing the ion source extraction aperture diameter to 50 μm greatly enhanced the ion-optical properties of the extracted beam.

**ORCID**
**Vitalii I. Voznyi**, https://orcid.org/0000-0002-9979-639X; **Aleksandr G. Ponomarev**, https://orcid.org/0000-0002-4517-5635
**Dmytro V. Mahilin**, https://orcid.org/0009-0005-7024-7142; **Dmytro P. Shulha**, https://orcid.org/0000-0002-4359-3446
**Volodymyr A. Rebrov**, https://orcid.org/0000-0002-4710-4670

**REFERENCES**
[1]  S. Matsuyama, M. Miwa, S. Toyama, T. Kamiya, Y. Ishii, and T. Satoh, Nucl. Instr. and Meth. B. **539**, 79 (2023). http://doi.org/10.1016/j.nimb.2023.03.023

[2] M. Jaksic, G. Provatas, I. Bozicevic Mihalic, A. Crnjac, D. Cosic, T. Dunatov, O. Romanenko, and Z. Siketic, Nucl. Instr. and Meth. B, **539**, 120 (2023). http://doi.org/10.1016/j.nimb.2023.03.031

[3] G. Nagy, H.J. Whitlow, and D. Primetzhofer, Nucl. Instr. and Meth. B, **533**, 66 (2022). http://doi.org/10.1016/j.nimb.2022.10.017

[4] A.G. Ponomarev, and A.A. Ponomarov, Nucl. Instr. and Meth. B, **497**, 15 (2021). http://doi.org/10.1016/j.nimb.2021.03.024

[5] S. Kalbitzer, Nucl. Instr. and Meth. B, **158**, 53 (1999). https://doi.org/10.1016/s0168-583x(99)00324-9

[6] J.A. van Kan, R. Pang, T. Basu, Y. Dou, Gokul, N. Tarino, J. Tregidga, *et al.* Rev. Sci. Instrum. **91**, 013310 (2020). https://doi.org/10.1063/1.5128657

[7] Y. Dou, T. Osipovicz, and J.A. van Kan, Ultramicroscopy, **253** 113812 (2023). https://doi.org/10.1016/j.ultramic.2023.113812

[8] V.I. Voznyi, A.G. Ponomarev, D.V. Mahilin, D.P. Shulha, and V.A. Rebrov, PAST, (3), 94 (2025). https://doi.org/10.46813/2025-157-094

[9] V.I. Voznyi, M.O. Sayko, A.G. Ponomarev, S.O. Sadovyi, O.V. Alexenko, and R.O. Shulipa, East Eur. J. Phys. (3), 46 (2020). https://doi.org/10.26565/2312-4334-2020-3-06

[10] P.W. Allison, J.D. Sherman, and D.B. Holtkamp, IEEE Trans. Nucl. Sci. **30**(4), 2204 (1983), https://doi.org/10.1109/TNS.1983.4332762

[11] C. Poggi, E. Sartori, M. Tollin, M. Brombin, M. Zaupa, E. Fagotti, and G. Serianni, Rev. Sci. Instrum. **91**, 013328 (2020). https://doi.org/10.1063/1.5129650

[12] J.D. Lawson, *The Physics of Charged Particle Beams*, 2nd ed. (Clarendon Press, Oxford, 1988), pp. 200.

[13] P.M. Lapostolle, IEEE Trans. Nucl. Sci. **18**(3), 1101 (1971). https://doi.org/10.1109/TNS.1971.4326292

[14] D.P. Moehs, J. Peters, and J. Sherman, IEEE Trans. Plasma Sci. **33**(6), 1786 (2005). https://doi.org/10.1109/TPS.2005.860067

[15] M. Reiser, *Theory and Design of Charged Particle Beams*, 2nd ed. (Wiley-VCH, Weinheim, 2008), pp. 53. http://dx.doi.org/10.1002/9783527622047

### ЕМІТТАНС ІОННОГО ВЧ ДЖЕРЕЛА МАЛОЇ ПОТУЖНОСТІ З МІКРОМЕТРОВИМ ЕКСТРАКЦІЙНИМ ОТВОРОМ

**Віталій І. Возний, Олександр Г. Пономарьов, Дмитро В. Магілін, Дмитро П. Шульга, Володимир А. Ребров**

*Інститут прикладної фізики НАН України, 58, вул. Петропавлівська, 40000 Суми, Україна*

Концепція компактного ядерного мікрозонда ґрунтується на використанні спеціалізованих джерел іонів зі струмом, що не перевищує декількох наноампер і малим розкидом по енергії. В ІПФ НАН України розроблено іонне ВЧ джерело для використання у компактному ядерному мікрозонді. Джерело працює при низькій ВЧ потужності < 10 Вт і призначене для генерації пучка іонів $^1H^+$, необхідного для стандартних методик, таких як PIXE, RBS та протонно-променева літографія. З метою зменшення еміттансу пучка та підвищення просторової роздільної здатності мікрозонда, діаметр екстракційного отвору джерела зменшено до 50 мкм. У роботі приводяться результати вимірювання загального струму та еміттансу пучка, який екстрагується з іонного ВЧ джерела малої потужності з мікрометричним екстракційним отвором. Наведено дані щодо вимірювання профілю пучка, його діаметра та кута розходження. ВЧ джерело має параметри: діаметр кварцової колби - 34 мм, довжина - 70 мм, робочий газ-водень, діаметр отвору екстракції – 50 мкм, ВЧ-потужність ≤10 Вт, частота - 45 МГц, іонний струм до 100 нА. Напруга екстракції змінюється від 10 до 300 В, енергія пучка 1-6,5 кеВ. Вимірювання еміттансу пучка проводилося за допомогою електростатичного сканера, виконаного за схемою Аллісона. Найменше значення еміттансу, що містить 90% повного струму пучка, дорівнює $\varepsilon_{90}$=1,36 $\pi$·мм·мрад, а rms-еміттанс- $\varepsilon_{rms}$=0,32 мм·мрад. Нормалізований еміттанс становить $\varepsilon_N$=0,003 $\pi$·мм·мрад, а енергетично нормалізований емітанс дорівнює 0,1 $\pi$·мм·мрад·(МеВ)$^{1/2}$. Таким чином, зменшення діаметра екстракційного отвору іонного джерела до 50 мкм призвело до помітного підвищення іонно-оптичних характеристик екстрагованого пучка.

**Ключові слова**: *іонний пучок; високочастотне джерело іонів; щільність струму пучка; екстрактор; еміттанс*